Catalysis Letters, Vol. 115, Nos. 3–4, June 2007 (© 2007)
DOI: 10.1007/s10562-007-9080-2

The effect of La on Au-ceria catalyst for water gas shift reaction

Qing Zhang, Yingying Zhan, Xingyi Lin, and Qi Zheng*

National Engineering Research Center of Chemical Fertilizer Catalyst, Fuzhou University, Fujian, Fuzhou 350002, P.R. China

Received 8 March 2007; accepted 8 March 2007

For Au-ceria catalysts prepared by deposition-precipitation method, catalytic performance of water gas shift reaction was studied in different La loadings. In the complete doping range, ceria retains with its cubic fluorite structures. BET, XRD, H_2-TPR, HRTEM studies showed that La doping can improve the activity of Au-ceria catalyst by stabilizing ceria and modifying its morphology. In addition, the test of catalyst stability evaluation also proved a better stability performance of Au-ceria catalyst can be realized by appropriate La doping.

KEY WORDS: Au-ceria catalyst; water-gas shift; La doping.

1. Introduction

Great intense developments are currently being made for polymer electrolyte membrane fuel cell (PEMFC) [1–4]. It has been proved [2] pure hydrogen system is not as practical as on-board hydrogen production. Thus, fuels such as methane, methanol or gasoline should be reformed to obtain a hydrogen-rich gas, and then further processed by a water-gas shift catalyst to maximize the yield of H_2 and reduce the CO concentration from ~10 to 1%, finally preferential oxidation of CO (PROX) takes over to further reduce the concentration to below 50 ppm, which can be tolerated by PEM fuel cells. Thus water-gas shift reaction play a significant role in the feasibility of mobile or small scale, local hydrogen generation.

CeO_2 nanoparticles, characterized by its high oxygen storage capacity, has lately been used as support for noble metal catalysts in variety of reactions, such as the water-gas shift reaction, the catalytic combustion of VOC, and the low-temperature CO oxidation [5]. Several studies [5–8] have shown that CeO_2 is an active support for water-gas shift reaction while the addition of gold further promotes this reaction [8]. However, the role of ceria as a support for noble metal-base catalyst is not only related to its high oxygen storage capacity but also to the improved dispersion of the noble metal and the promotion of the WGS reaction [9].

It has been reported that the rare earth additives can improve the properties of the catalysts and decrease the consumption of precious metals at the same time [10]. Fu et al. had found in their work [7] that certain dopants, such as lanthana, can stabilize ceria and prevent its sintering. Recently, S. Patil et al. [11] found the size dependent lattice expansion, induced by increasing oxygen vacancies in CeO_2 nanoparticles can be further increased by La^{3+} dopant. Sanchez and Gazquez [12] proposed that oxygen vacancies in the fluorite oxide structure in supported catalysts alter the morphology and dispersion of the supported metal. For better understanding the effect of the lanthana on Au/CeO_2, we prepared a series of Au-ceria catalysts with La_2O_3doping by deposition precipitation method. Specifically, the activity and stability of the catalysts in realistic fuel gas mixtures were also investigated.

*To whom correspondence should be addressed.
E-mail: qizheng2005@gmail.com

2. Experimental

2.1. Catalyst preparation

For deposition-precipitation method, the supports were ceria doped with different content La, and prepared from aqueous solution of $Ce(NO_3)_3 \cdot 6H_2O$ and $La(NO_3)_3 \cdot 6H_2O$ by co-precipitation method. In brief, metal nitrate aqueous solutions were mixing with K_2CO_3 at 60–70 °C, keeping pH between 8–10 and aging the precipitate at 60–70 °C for 1 h. Further, the precipitate was dried over night at 110°C and calcined in static air at 400°C for 2 h.

The gold-ceria samples with La doping used in this method were designed to load 3 wt% Au. For example, the sample without La doping is noted as ACL0. Besides, the 5ACL0 sample which is designed to load 5 wt% Au and without La doping is prepared for stability test After calcination, the support was crushed into fine particle, and thoroughly suspended in deionized water under ultrasound irradiation. Then, add the desired amount of $HAuCl_4$ dropwise into aqueous slurry of prepared ceria at 60 °C. The pH of the slurry was

adjusted to the value of nine using ammonium hydroxide. The resulting precipitate was aged at the same temperature for 4 h and then washed with deionized water until there were no residual Cl^- ions as tested by 0.1 M $AgNO_3$ solution. Then the precipitate was dried at 100–120 °C and calcined in static air at 300 °C for 4 h.

2.2. Catalytic activity measurement

The catalytic tests for WGS reaction was carried out in a commercial fixed-bed reactor (CO-CMAT9002, HD Co. Ltd., PeiKing, PRC) at atmospheric pressure over a wide temperature range (200-450 °C). The total time on stream was about 18 h. A stainless steel tube with an inner diameter of 9 mm was chosen as the reactor tube [13]. All samples were sieved to 450∼700 um. The sample weight was 0.40–0.60 g (0.5 cm^3) and gas hourly space velocity of the reactant mixture was 10000 h^{-1}, and all samples were used without activation. Water was injected into the flowing gas stream by calibrated syringe pump and vaporized in the vaporizer(100 °C) before entering the reactor. Two kinds of feed gas were used in the test, one mixture typically contained 10 vol.% CO diluted by nitrogen; another gas composition simulating realistic fuel gas mixtures was 5% CO, 6%CO_2, 31.6%H_2, 9.5%N_2 and 46.5% steam. A condenser was installed at the reactor exit to collect water. The product was analyzed using an on-line gas chromatograph (Shimadzu GC-8A) equipped with a thermal conductivity detector. The CO conversion was calculated as follows: $X(CO)(\%) = (1-V'_{co}/V_{co}) \times 100\%/ (1 + V'_{co})$.

After the test, the stream was shut down and catalysts were cooling down to room temperature in N_2.

2.3. Characterization of catalysts

The BET specific surface areas and the pore volume were determined from adsorption and desorption isotherms of nitrogen at −196 °C using a Quantachrome NOVA 4200e apparatus. All samples were degassed under vacuum at 200 °C for 4 h.

XRD analyses of powders were carried out on a PANalytical X'Pert PRO MPD Multi-Purpose Diffractometer System with X'Celerator Detector, operating voltage of 40 kV and current of 40 mA, using Co Ka radiation (0.1789 nm). The angular range varied from 20° to 80°, with increments of 0.033° and counting time of 60 s per step. The crystal size of ceria and gold was calculated from FWHM using the Scherrer equation.

Temperature-programmed reduction (TPR) characterization was carried out in a Micromeritics Autochem 2910 instrument. Over 100 mg of the fresh sample was packed into a reactor with quartz tubing of 6 mm id., and was first purged with high purity helium gas at 150 °C for 1 h, cooled down to room temperature. TPR traces of sample was then pursued in a reductive flow of 30 ml/min 10 vol.%H_2 in helium, heated at a rate of 5 °C/min from room temperature to 900 °C. The rate of hydrogen consumption was monitored by TCD of instrument.

High resolution transmission electron microscopy (HRTEM) analysis was performed using a JEOL 2010F (200 kv) microscope equipped with an EDS analytical system Oxford Link. The powered samples were ultrasonically dispersed in ethanol and the obtained suspensions were deposited on a copper grid, coated with a porous carbon film.

3. Results and discussion

The X-ray diffraction patterns of synthesized samples were shown in figure 1. Respective of the formulas, all samples have distinct crystal phases of fluorite oxide-type CeO_2. A slight shift to lower angles was observed, from 33.04°to 32.86°, as La content being increased. Such shift is usually related to the addition of promoters[11] to CeO_2 can result in an increase in lattice spacing of CeO_2, which due to the incorporation of the promoter or metal into the CeO_2 lattice. The lattice constant variation of cubic ceria for samples as a function of doping amount of La was provided in figure 2. It showed the increase in the lattice constant with the La dopant concentration. This proved the ion of La^{3+} (0.116 nm) submits into the lattice of ceria. Even in high content sample, no separate reflections from La_2O_3, this probably attributes to La forms some kinds of oxide solid solution with ceria. And a small broad peak corresponding to Au(111) was seen in the as prepared samples. With increasing La loading, ceria particle size decreased gradually and the gold diffraction peaks changed very slightly, the gold particle size showed in table 1, almost unchanged, which indicated a strong interaction between gold and support.

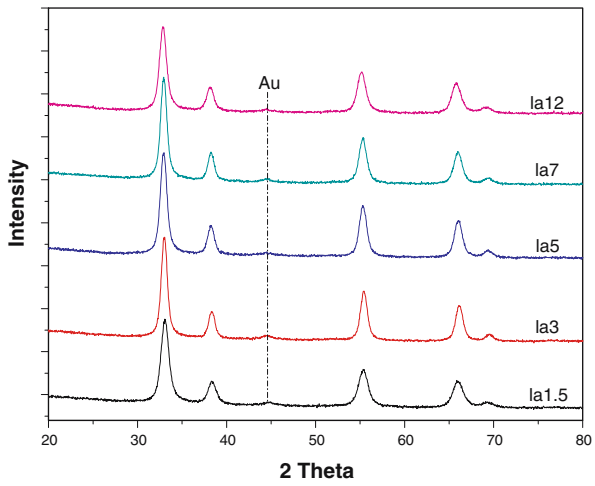

Figure 1. X-ray diffraction patterns for samples with different La doping.

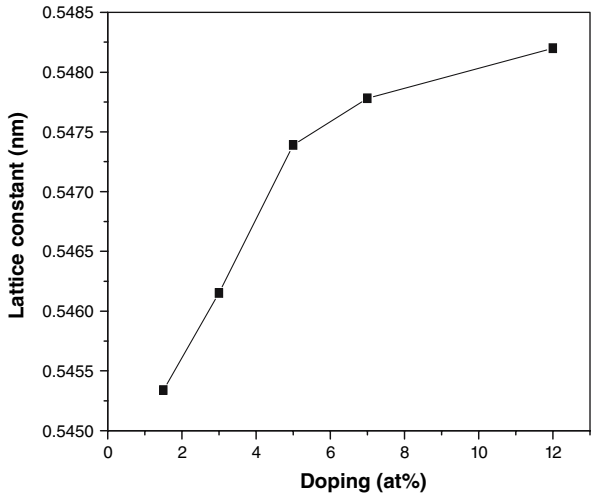

Figure 2. Lattice constant variation of the fresh samples as a function of doping amount.

The activity data of the samples with different La content, measured in the temperature range 200–450 °C was summarized in figure 3. A trend of the conversion of CO increasing by La doping was present in all catalysts. And the conversion of CO was greatly increasing between 200–300 °C,and slow down to reach a maximum at 400 °C. Especially, the catalyst with 5 at% La loading (Au/CL5) showed the highest CO conversion and it divided the other samples into two groups. In lower La content samples (below 5 at%), apparently increase of catalytic activity was showed with increasing La loading. On contrast, the catalytic activity decreased gradually for further increase the La loading. The surface area and porous structure properties for La doped Au/ceria catalysts were present in table 1. The surface area increased gradually as La loading increasing; it increased 34.5% when La concentration reached 7 at%. But the sample(Au/CL7)with highest surface area did not show the best activity, that means the surface area not linear correlate with catalytic activity. And interestingly, a trend of slightly decrease of ceria particle size and cumulative pore volume were showed with La doping. Above all, low content La for improving catalytic activity was benefit with surface area increasing and ceria particle size decreasing.

The typical TPR profile of cerium oxide support with various La doping was shown in figure 4a. One shoulder and two reduction peaks with higher intensity at about 300, 450 and 700 °C were presented, the former two were assigned to ascribe to the reduction of surface and subsurface ceria, and the later is assigned to bulk oxygen reduction in support. [14] For all the samples examined, these two characteristic peaks were observed being shift to lower temperature at the presence of La. As La content increasing from 1.5–12 at%, the first peak with a maximum shift from 488–430 °C, and T_{max} of the second one shift from 776–683 °C. Such enhanced reduction behavior proved the La^{3+} submitted into the lattice of ceria and improved it reduction properties.

A phenomenon of the gold function catalyzes and thereby shifts the peak for the reduction of surface shell of ceria to lower temperature is proved in figure 4b. Obviously, the reduction of surface oxygen in ceria was substantially improved by the presence of gold, its T_{max} lowered by several hundred degrees. Comparing to the blank sample ACL0, the reduction peaks of surface oxygen in ceria of La doping samples were shift from 100 °C to about 60°C. It can be derived from the width of the reduction peak of surface capping oxygen of ceria that Au/CL5 processes the best uniformity since its corresponding peak is symmetric with a maximum at 82.8 °C. Calculating the area of the first reduction peak, it is found that the Au/CL5 has the second largest H_2 consumption (96 μmol/g_{cat}). Combined with the result obtained above, we can conclude that Au/CL5 not only have nanosize gold particles, but also process the interaction between nanosized gold particles and ceria with optimal La loading, leading to its highest activity.

The bright-field HRTEM image of Au/CL5 catalyst in figure 5 exhibit near-spherical ~10 nm particles of

Table 1
Microstructure properties for samples

Sample	S_{BET} (m^2/g)		Particle size /nm			Lattice constant		Average pore size(nm)	Cumulative pore volume(cm^3/g)
	Fresh	Spent	Au	CeO_2		α/Å[a]	CeO_2		
			111	(111)	(200)	(111)	(200)		
Au-ceria	65	ND[b]	ND	14.1	14.9	5.410	5.406	13.23	0.17
Au/CL1.5	72	66	6.0	13.5	13.6	5.453	5.451	13.24	0.21
Au/CL3	80	59	5.9	13.1	13.3	5.462	5.461	8.58	0.17
Au/CL5	83	57	5.8	12.9	12.8	5.474	5.472	10.48	0.17
Au/CL7	97	44	6.0	11.6	11.4	5.478	5.475	6.78	0.13
Au/CL12	93	56	6.3	10.5	10.6	5.482	5.478	8.66	0.12

[a]The lattice constant α was determined by the expression $\alpha = sqrt(h^2 + k^2 + l^2)(\lambda/2\sin\theta)$
[b]ND: Not detected.

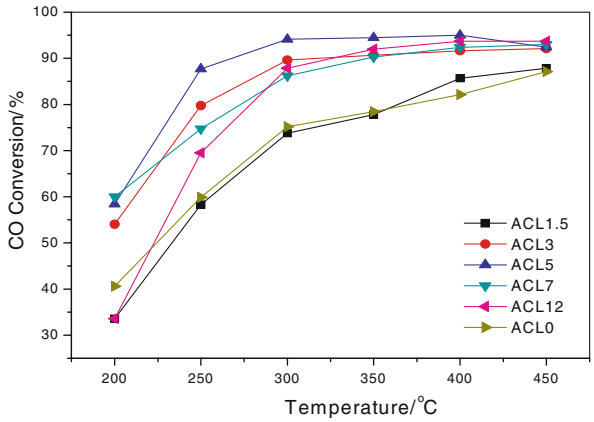

Figure 3. Temperature dependence of WGS activity of Au/CL samples with different La doping. reactants:10%CO in N_2; space velocity: 10000 h^{-1}; steam gas ratio: 0.9 : 1.

ceria with a uniform particle distribution. The SAED pattern shown in the inset of the micrographs identifies the nanocrystalline ceria with fluorite crystal structure. And it found that gold particles in the sample have an average size of 6 nm, which was in agreement with the result measured by XRD.

Catalyst stability evaluation is important both to improve fundamental understanding of the activity, and to enable practical catalyst designs. Thus, in the present work we conducted the test to check the stability of Au/CL catalyst in simulating realistic fuel gas mixtures containing 5% CO, 6%CO_2, 31.6%H_2, 9.5%N_2 and 46.5% steam. Two kinds of Au-ceria catalysts with the same activity in 300 °C(space velocity 20000 h^{-1}) were compared in figure 6. In the first 3 h, two samples deactivated with almost the same speed. After that, the sample without La doping (5AuCL0), deactivated much faster, its activity decreased to about 45% after 14 h test. On contrary, the 3AuCL5 sample present more stable properties and its activity kept constant at about 65% in the test. Obviously, the doping of La improved the stability of Au-ceria catalyst and decreases the consumption of precious metals at the same time. For ceria supported catalysts, Fu et al. found[15] the addition of La inhibited the crystal growth of ceria in

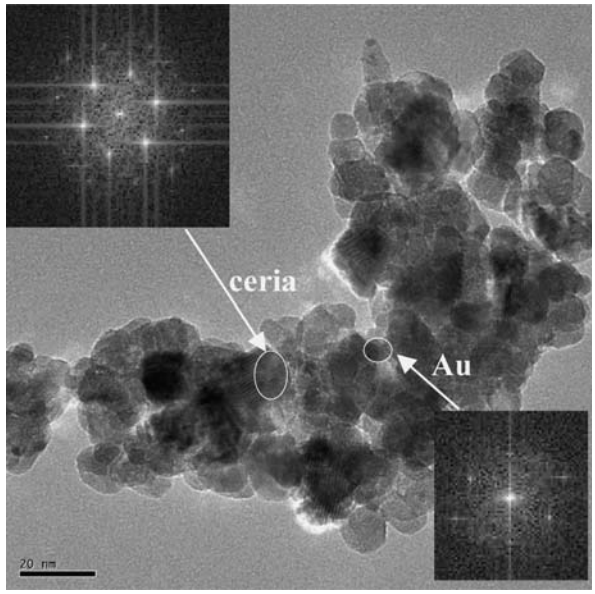

Figure 5. HRTEM image of as prepared Au/CL5 sample at an original magnification of 500,000 ×.

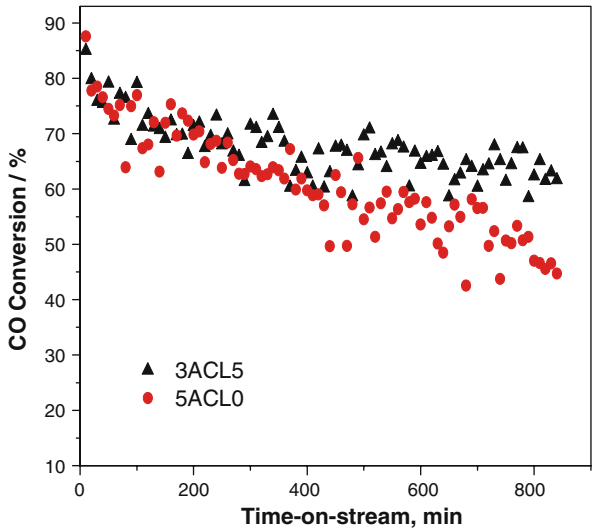

Figure 6. Stability of gold-ceria WGS catalysts.Space velocity: 20,000 h^{-1} (NTP); 5% CO, 6%CO_2, 31.6%H_2, 9.5%N_2 and 46.5% steam; reaction temperature: 300 °C.

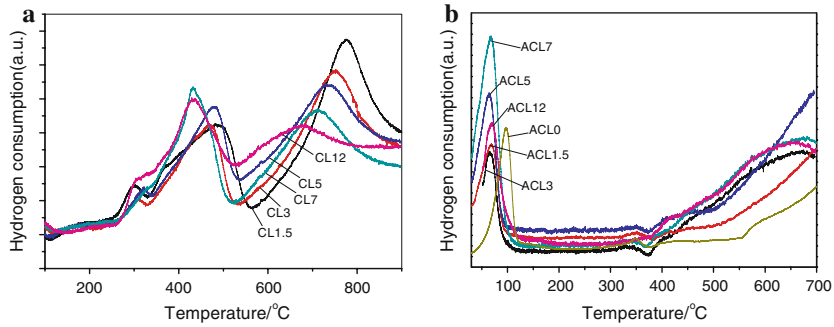

Figure 4. H_2-TPR profiles of CeO_2–La_2O_3 (a) and ceria-based catalysts (b) with different La_2O_3 loading; 10%H_2/He, 30cm^3/min(NTP), 5°C/min.

catalysts made by different preparation methods. And Li [16] and their co-workers sucessfully used Lanthanum dopnat(10 at.%) as a structure stabilizer of ceria in their research work. From these reports, it is obvious that La doping can modify the morphology of ceria and make it more stabilizing. However, the nature of deactivation of Au-ceria catalyst is still not clear, and the interaction between lanthana and Au required further investigation.

4. Conclusions

Based on the studies of structure and properties of Au-ceria catalyst, it is well established that La doping can improve the activity of Au-ceria catalyst by stabilizing ceria and modifying its morphology. Besides, the test of catalyst stability evaluation also proved a better stability performance of Au/ceria catalyst can be realized by La doping. However, the nature of deactivation of Au-ceria catalyst is still not clear, and further studies will lead to a more thorough understanding of the unique catalytic of Au-ceria catalysts.

Acknowledgments

The financial support of this work by National Science Council of the Republic of China through contact No. 20271012, is gratefully acknowledged.

References

[1] Fuel Cell Handbook, fifth ed., US DOE, NETL, 2000.
[2] S.L. Swartz, M.M. Seabaugh, C.T. Holt and W.J. Dawson, Fuel Cell Bull. 30 (2001) 7.
[3] D. Cameron, R. Holliday and D. Thompson, J Power Sources 118 (2003) 298–303.
[4] Fuel Cells for Transportation Program Contractors' Annual Progress Report, US DOE, OAAT, 1998.
[5] A.M. Venezia, G. Pantaleo, A. Longo and G.D. Carlo, J Phys Chem B 109 (2005) 2821–2827.
[6] S. Letichevsky, C.A. Tellez, R.R. Avillez and L.G. Appel, Appl Catal B Environ. 58 (2005) 203–210.
[7] Q. Fu, A. Weber and M. Flytzani-Stephanopoulos, Catal Lett. 77((1–3) (2001) 87.
[8] X. Liu, W. Ruettinger, X. Xu and R. Farrauto, Appl Catal B Environ. 56 (2005) 69–75.
[9] T. Venkov, H. Klimev, M.A. Centeno, J.A. Odriozola and K. Hadjiivanov, Catal Comm. 7 (2006) 308–313.
[10] M. Ozawa, O. Kato and S. Suzuki, J Mater Sci Lett. 15 (1996) 564–569.
[11] S. Patil, S. Seal, Y. Guo, A. Schulte and J. Norwood, Appl Phys Lett. 88 (2006) 243110.
[12] M.G. Sanchez and J.L. Gazquez, J Catal. 104 (1987) 120.
[13] J. Hua, Q. Zheng, Y. Zheng, K. Wei and X. Lin, Catal Lett. 102(1–2) (2005) 99–108.
[14] L.F. Liotta, G. Pantaleo, A. Macaluso, G. Marcì, S. Gialanella and G. Deganello, J Sol-Gel Sci Tech. 28 (2003) 119–132.
[15] Q. Fu, S. Kudriavtseva, H. Saltsburg and M. Flytzani-Stephanopoulos, Chem Engi J. 93 (2003) 41–53.
[16] Y. Li, Q. Fu and M. Flytzani-Stephanopoulos, Appl Catal B Environ. 27 (2000) 179.